The EMBO Journal vol.13 no.24 pp.6011–6020, 1994

p53 oligomerization and DNA looping are linked with transcriptional activation

Judith E.Stenger[1], Peter Tegtmeyer, Gregory A.Mayr, Michael Reed, Yun Wang, Pin Wang, Paul V.C.Hough[2] and Iris A.Mastrangelo[2,3]

Department of Molecular Genetics and Microbiology, State University of New York, Stony Brook, NY 11794 and [2]Biology Department, Brookhaven National Laboratory, Upton, NY 11973, USA
[1]Present address: Laboratory of Molecular Carcinogenesis, National Institute of Environmental Health Sciences, Research Triangle Park, NC 27709, USA

[3]Corresponding author

Communicated by R.Knippers

We examined the role of p53 oligomerization in DNA binding and in transactivation. By conventional electron microscopy (EM) and scanning transmission EM, we find that wild-type tetramers contact 18–20 bp at single or tandem 19 bp consensus sequences and also stack in apparent register, tetramer on top of tetramer. Stacked tetramers link separated DNA binding sites with DNA loops. Interestingly, the p53(1–320) segment, which lacks the C-terminal tetramerization domain, binds DNA consensus sites as stacked oligomers. Although the truncated protein binds DNA with reduced efficiency, it nevertheless induces DNA looping by self-association. p53, therefore, has a C-terminal tetramerization domain that enhances DNA binding and a non-tetrameric oligomerization domain that stacks p53 at consensus sites and loops separated consensus sites via protein–protein interactions. Using model promoters, we demonstrate that wild-type and tetramerization-deficient p53s activate transcription well when tandem consensus sites are proximal to TATA sequences and poorly when tandem sites are distal. In the presence of proximal sites, however, stimulation by distal sites increases 25-fold. Tetramerization and stacking of tetramers, therefore, provide dual mechanisms to augment the number of p53 molecules available for activation through p53 response elements. DNA looping between separated response elements further increases the concentration of local p53 by translocating distally bound protein to the promoter.

Key words: electron microscopy/oligomerization/p53/transactivation/tumor suppressor

Introduction

Inactivation of the p53 tumor suppressor gene plays a major role in the development of many human cancers (Vogelstein and Kinzler, 1992). Characteristically, mutant p53 proteins in tumors lack specific DNA binding activity (Bargonetti *et al.*, 1991; Foord *et al.*, 1991; Hollstein *et al.*, 1991; Kern *et al.*, 1991a). p53 contains an acidic transactivation domain and regulates transcription, *in vivo* and *in vitro*, by site specific DNA binding to a 20 bp palindromic sequence (Fields and Jang, 1990; Raycroft *et al.*, 1990; Kern *et al.*, 1991b; El-Deiry *et al.*, 1992; Farmer *et al.*, 1992; Funk *et al.*, 1992; Scharer and Iggo, 1992; Unger *et al.*, 1992; Zambetti *et al.*, 1992). In addition to its activator function, p53 can also repress promoters that lack p53 binding sites but contain TATA elements (Ginsberg *et al.*, 1991). p53 binding interactions with TBP, the TATA binding protein subunit of basal transcription factor TFIID, may be involved in this repression (Seto *et al.*, 1992; Mack *et al.*, 1993; Ragimov *et al.*, 1993; Truant *et al.*, 1993). In contrast, at promoters containing p53 binding sites and the TATA element, p53 and TFIID bind cooperatively, suggesting that p53 activates transcription by stabilizing the TFIID–TATA complex (Chen *et al.*, 1993; Liu *et al.*, 1993). Wild-type p53 activates a number of cellular genes including the *WAF1/Cip1* gene whose product itself suppresses cell growth by strongly inhibiting several G_1-phase cyclin-dependent kinases required for entry into S phase (El-Deiry *et al.*, 1993; Harper *et al.*, 1993). The identification of this target gene provides a mechanistic link between p53 functions in transcription and tumor suppression.

In natural promoters, p53 response elements are often located at significant distances from TATA sequences. In the WAF1 promoter, two 20 bp consensus sequences are located between 2 and 3 kb upstream of the transcription start site (El-Deiry *et al.*, 1993; B.Vogelstein, personal communication). A third p53 site, with partial matches to repeated consensus sequences, is located at −75 bp relative to the start site. An extended 50 bp p53 response element with partial homology to the consensus sequence is found 3 kb upstream of the *MCK* gene (Weintraub *et al.*, 1991; Zambetti *et al.*, 1992). Two consensus sequences confined within 85 bp are located in an intron 1.5 kb downstream from the start site of the *MDM2* gene (Wu *et al.*, 1993), and, in the *GADD45* gene, a 20 bp response element is located in an intron 500 bp downstream from the start site (Kastan *et al.*, 1992). In model promoters, natural p53 binding sites placed adjacent to TATA elements effectively stimulate transcription by p53. It seems likely, therefore, that p53 stimulates transcription both as a local activator and by distal enhancer activity.

The occurrence of distal binding sites in natural genes raises the possibility that p53 may interact with promoter regions via DNA loops and that this geometry may be important in transactivation (Ptashne, 1986; Wolffe, 1994). Other activator proteins stimulate transcription synergistically through the mediation of loop structures between proteins bound at well-separated DNA sites (Knight *et al.*, 1991; Li *et al.*, 1991; Mastrangelo *et al.*, 1991; Su *et al.*, 1991; Beachy *et al.*, 1993). Multimeric structures, such

as homo-multimers of E2 dimers and of Sp1 tetramers, frequently assemble at loop junctures (Knight *et al.*, 1991; Mastrangelo *et al.*, 1991). Hetero-multimers in loop structures that join widely separated E2 and Sp1 proteins are also associated with synergistic activation (Li *et al.*, 1991). Purified p53 exists as tetramers and multiples of tetramers in the absence of DNA (Stenger *et al.*, 1992; Friedman *et al.*, 1993). Either of these oligomeric forms could have DNA binding domains available for simultaneous interaction with separated DNA sites.

Our aim in this work was to elucidate the effects of oligomerization on functional interactions of p53 with its DNA binding element. We examined DNA–protein structures assembled by wild-type p53 and tetramerization-deficient p53 using conventional electron microscopy (EM) and scanning transmission EM with molecular mass determination (STEM). In a model promoter containing multiple copies of the consensus sequence, we found that both wild-type tetramers and tetramerization-deficient p53 assemble oligomeric masses by a previously unreported stacking mechanism. Stacked oligomers of each protein also link separated binding sites via DNA loops. We present evidence that p53 stacking at consensus binding sites or linking of two widely separated binding sites by tetramer–tetramer interactions are associated with enhanced transcription *in vivo*. The observed strong correlation between DNA binding structures and enhanced transactivation suggests that both tetrameric and non-tetrameric oligomerization, with and without DNA looping, will be found to mediate p53 function in natural promoters.

Results

Wild-type p53 links 13RE sites to form small and large loops

For EM studies of DNA binding and for transactivation studies, we used 13 tandem copies of the 19 bp RGC site as a p53 response element (13RE). We chose this DNA for a number of reasons. Kern *et al.* (1991b, 1992) showed that this segment promotes high levels of transcription in a dose-related manner that exceeds a linear response. One-half of each RGC site exactly matches and the other half shows close correspondence with the 5′-PuPuPuC(A/T)(A/T)GPyPyPy-3′ motif present as two copies in the p53 consensus sequence (El-Deiry *et al.*, 1992). Therefore, it is a representative binding sequence given the range found among natural sequences. The tandem repeats also provide a very sensitive assay for DNA looping. Finally, results using single p53 consensus sequences are qualitatively similar to those using tandem consensus sites (see below).

Binding conditions used for our EM studies were tested using DNase I protection assays. We adapted conditions under which purified p53 gave complete protection of a single copy of the RGC site in the absence of competitor DNA and other proteins (data not shown). In the p13RE$^{PROX/DIST}$ plasmid DNA, a proximal 13RE is present 25 bp upstream of the E1b TATA sequence and is separated by 1700 bp from a second, distal, 13RE (Figure 1A). The histogram in Figure 1B quantitates the frequency of p53 binding along the *Afl*III-cut plasmid and shows that wild-type p53 bound predominantly, though not exclusively, at the two 13RE sites, and in approximately equal quantities.

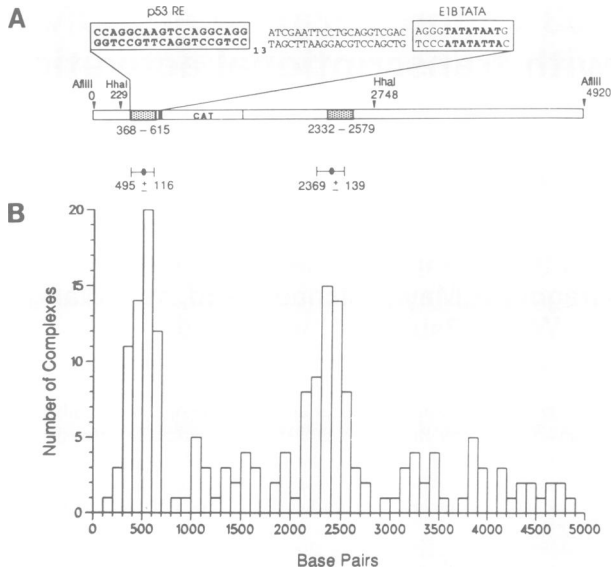

Fig. 1. Binding positions of p53 complexes on DNA, observed by conventional EM, coincide with the 13RE consensus sequences. (**A**) Schematic diagram of the 4920 bp reporter plasmid p13RE$^{PROX/DIST}$, linearized by *Afl*II for use as a binding substrate. *Hha*I cutting sites are also indicated. Sequences of the proximal and distal 13RE sites (dotted rectangles), the E1b TATA box (black rectangle), and the intervening polycloning site are shown. The reporter chloramphenicol acetyltransferase (*CAT*) gene is adjacent to TATA and separated from the distal 13RE site by the SV40 small t splicing and polyadenylation signals. Proximal and distal 13REs extend 247 bp with centers at 492 and 2456 bp, respectively. The center of the distal site is within 0.2% of the center of the *Afl*III fragment. Digestion by *Hha*I produces a 2519 bp fragment with the proximal and distal 13REs almost equidistant from each *Hha*I end. (**B**) The histogram shows centers of binding positions occupied by p53 complexes on *Afl*III–p13RE$^{PROX/DIST}$ DNA. Positions were measured from the nearest DNA end. Most fragments with non-specific binding also had specific binding. Sites of non-specific binding were measured correctly when present with proximal site binding. Sites of non-specific binding, when present with binding at the distal site or on DNAs with purely non-specific binding, were measured randomly from either end. Actual lengths measured in bp were multiplied by 1.15 in order to normalize the mean length for all fragments to 4920 bp. Ellipses with horizontal bars give the mean ± standard deviations (SD) for measurements at the proximal and distal REs.

Of the total p53 molecules associated with DNA, 73% bound at the response elements (Table I).

Conventional electron micrographs show that wild-type p53 binds as minimum complexes of one or two p53 molecules, as multiple tandem p53 molecules, and as higher-order associations linking proximal 13RE to distal 13RE sites via intersite DNA loops (Figure 2A and B; Table I). These different binding forms occur with approximately equal frequencies suggesting that co-operativity in binding to adjacent consensus sequences is not strong. Comparison of p53 molecules bound to DNA and found free on the thin carbon in the same fields of view indicate that p53 proteins frequently associate with the DNA as larger units. Contour lengths of intersite loop structures measured close to 34% of the *Afl*III DNA length, the expected distance between the 13RE sites (Figure 2A). Within a 13RE site, protein–protein contacts formed intrasite loop structures and joined very short DNA segments consisting of as little as 60 bp (Figure 2A; Table I). Hemi-specific loops between 13RE sequences and non-consensus sequence DNA were also formed

Table I. Binding of p53 to linearized plasmid DNA

	Wild-type p53[a]	p53(1–320)[b]
Total number of DNA fragments	120	459
Fragments with p53 bound (% of line above)	112 (93%)	188 (41%)
p53 at one or both 13RE sites	88 (73%)[c]	119 (26%)
p53 at both 13RE sites (% of line above)	28 (32%)	10 (8%)
Loops between proximal and distal 13RE sites (% of line above)	14 (50%)	5 (50%)
Intrasite or hemi-specific loops[d] (% of line 3)	14 (16%)	17 (14%)
Non-specific loops (% of line 1)	1 (1%)	0 (0%)

Observation by conventional EM
[a]*Aff*III–p13RE$^{PROX/DIST}$ DNA was used in the binding reaction at a stoichiometry of 25 monomers to one DNA.
[b]The *Hha*I–p13RE$^{PROX/DIST}$ fragment was used at a stoichiometry of 50 monomers to one DNA.
[c]60 or 51% of the p53 oligomers specifically bound were positioned at the proximal RE; 57 or 49% were at the distal RE.
[d]Intrasite loops occur within a single 247 bp 13RE binding site. Hemi-specific loops link a specific binding site and non-consensus sequence DNA. We observed two wild-type p53 and three p53(1–320) intrasite loops and additional intrasite loops by STEM (see Figure 4A).

(Table I). Only one loop joining two non-specific binding sites was observed. We conclude that p53 bound to separated DNA recognition sites self-associates to form DNA loops measuring from 60 to 1700 bp. Furthermore, the formation of p53 loop structures is very efficient even over long distances on linear DNAs (50%; Table I).

p53 binding at separated single consensus sequences loops DNA

We also examined p53 binding to a non-RGC consensus sequence in a relaxed, circular plasmid, pJSJS. This plasmid contains two single copies of a 20 bp consensus sequence, p53CON (Funk *et al.*, 1992), separated by 824 bp. Among 30 plasmids that had p53 complexes bound at both p53CON sites, 28 plasmids had specific loops (Figure 2D and data not shown). For 13RE DNAs, the comparable looping frequency was 50% (Table I). The higher frequency of p53CON loop formation reflects more closely spaced binding sites and the greater likelihood of contact in closed-circular substrates (Shore *et al.*, 1981). Link structures between the two p53CON sites, like those between 13RE sites, were typically larger than twice the size of free, unbound protein despite the presence of only a single copy of the consensus sequence in each site (Figure 2D). Such additional quaternary associations, localized at the loop junction, suggest that oligomerization is associated with DNA binding and the linking interaction.

Truncation mutant p53(1–320) also loops DNA

In order to determine whether link formation required the C-terminal tetramerization domain in p53, we examined DNA binding by the truncation mutant p53(1–320) which lacks the domain (Pavletich *et al.*, 1993; Wang *et al.*, 1994). This and similar mutants are mainly monomeric in solution but are still able to activate transcription (Foord *et al.*, 1991; Milner *et al.*, 1991; Sturzbecher *et al.*, 1992; Shaulian *et al.*, 1993; Wang *et al.*, 1993). By EM on *Hha*I plasmids, we find the binding frequency for p53(1–320) at 13RE sites to be 26%, almost three times lower than the frequency for wild-type p53 (Table I). Surprisingly, as observed for wild-type p53, p53(1–320) associated with 13RE sites appeared larger than free protein and also produced specific loop structures (Figure 2C; Table I). Although binding frequency was lower, the frequency of specific and hemi-specific p53(1–320) loops, expressed as a percentage of specific binding, was similar to that of wild-type p53 (Table I). In the case of p53(1–320), protein–protein associations in DNA binding and loop formation are independent of the C-terminal tetramerization domain. The formation of link structures and the assembly of large masses at loop junctures by wild-type p53, therefore, may also be distinct from the tetramerization function. This further capacity for oligomerization, beyond tetramer formation, would reside in amino acids 1–320 (Wang *et al.*, 1994).

Oligomerization of p53 and p53(1–320) by stacking in the absence of DNA

To understand the role of oligomerization in DNA binding, we used STEM molecular mass measurements to determine the oligomeric forms of wild-type p53 and p53(1–320) present in purified protein prior to binding DNA. Our results indicate that both proteins in the absence of DNA undergo additional oligomerization by a mechanism that involves similar protein–protein interactions between wild-type tetramers and between (1–320) monomers.

STEM mass profiles for p53 and p53(1–320) proteins are given in the histograms in Figure 3A and B, respectively. In panel A, the mean of the Gaussian fitted to the main peak corresponds to 4×43.5 kDa, the protein sequence mass for a p53 tetramer. The lower-mass shoulder on the tetramer peak may be composed of dissociating tetramers. Octamer masses form a small, independent group. These data agree with our previous observation of p53 tetramers and multiples of tetramers using gel electrophoresis (Stenger *et al.*, 1992). In panel B, the mean of the main peak corresponds to 38 kDa, the protein sequence mass for a p53(1–320) monomer. Two additional peaks represent dimers and trimers. Identification of dimer and trimer classes, not previously reported, can be attributed in part to the sensitivity and resolution of the STEM measurement. Absence of tetramer masses confirms that efficient tetramer formation requires the C-terminal residues.

In addition to mass measurements, STEM scattered electron counts show, in projection, mass contours within individual complexes (Hough *et al.*, 1984; Mastrangelo *et al.*, 1989). Unlike total mass determination, the projected mass contour, or mass thickness, depends on molecular orientation. Molecular mass thickness can be represented as the linear thickness of compact protein with increments indicated by color changes (described in the legend to

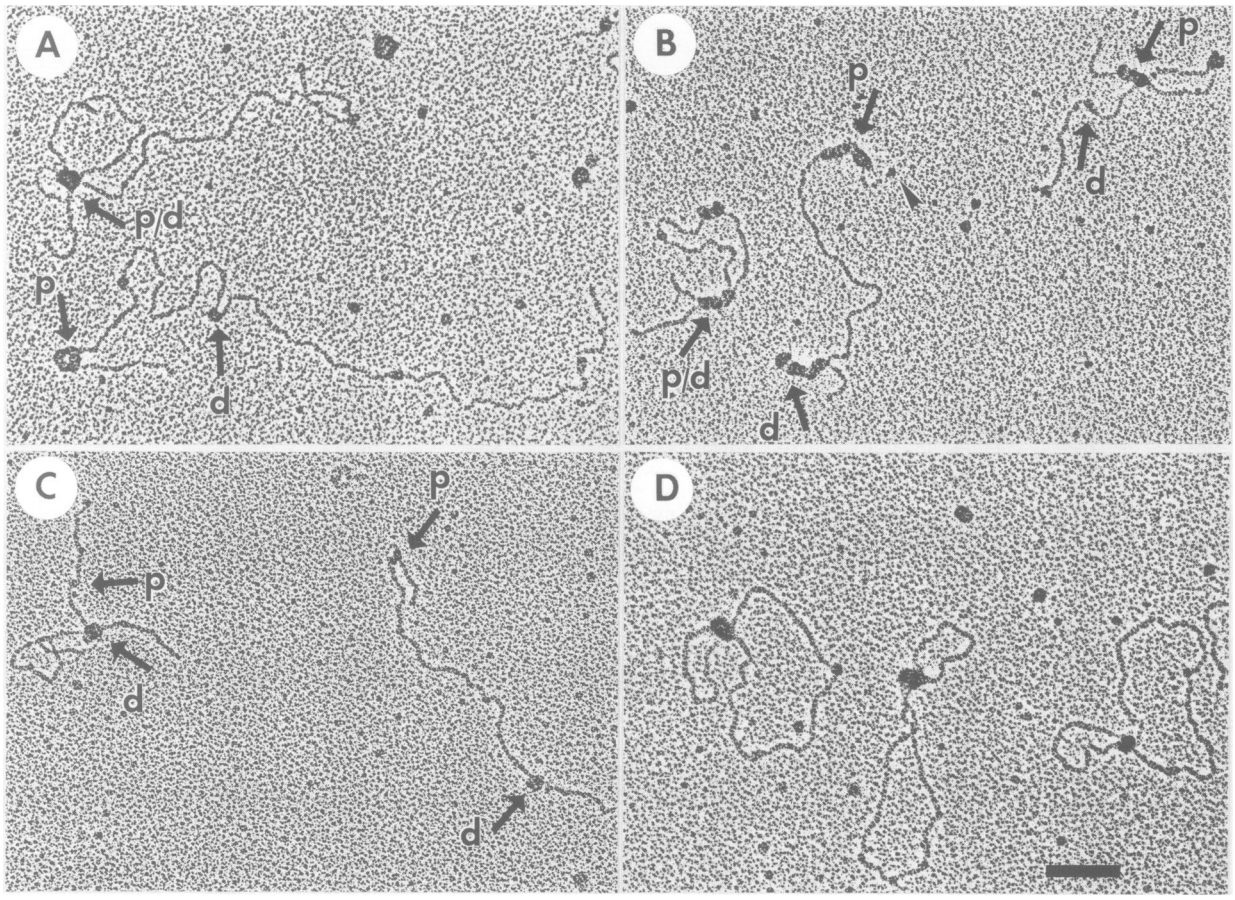

Fig. 2. Wild-type p53 and p53(1–320) assemble both unlinked and linked structures at 13RE sites and single consensus sequence binding sites, as observed by conventional EM. Bar represents 100 nm. Binding substrates are p13RE$^{PROX/DIST}$, linearized with *Afl*III (**A**) or with *Hha*I (**B** and **C**), and the relaxed pJSJS plasmid (**D**). 'p' and 'd' arrows indicate unlinked structures at proximal or distal 13RE sites; 'p/d' arrows indicate intersite loop structures. (A) Wild-type p53. A specific intersite loop (p/d) occupies the upper molecule. A proximal intrasite loop (p) and an unlinked distal complex (d) are present in the bottom DNA. (B) Wild-type p53. The left DNA shows an intersite loop (p/d). The center DNA has two unlinked specific complexes each extending close to 200 bp (p,d). An arrowhead indicates the DNA end. The right DNA has a small (d) and a large (p) specific complex. The large complex appears to cross over the DNA and was scored as an unlinked complex. (C) p53(1–320). On the left, a large hemi-specific link structure (d) and a small specific complex (p) assemble on the same fragment. On the right, two small assemblies link 60 bp in an intrasite loop (p) upstream from a large unlinked complex (d). (D) Wild-type p53. Three large oligomeric structures link two 20 bp consensus sequences.

Figure 3). Most tetramers and octamers are observed in orientations similar to those shown in the color panel in Figure 3A. Mass thickness in the octamer extends to the second purple band at 72 Å, double the thickness reached by the tetramer at the first purple band. A 2-fold increase in mass thickness suggests that octamers assemble by tetramer-on-tetramer stacking via contacts beyond those required for tetramerization. In the color panel in Figure 3B, p53(1–320) monomer to dimer to trimer increments in mass thickness average about 15 Å suggesting that two and three p53(1–320) monomers are stacked approximately in register one upon another.

Multiples of p53 tetramers bind at 13RE sites

STEM mass measurements of wild-type p53 bound at both linked and unlinked 13RE sites are presented in Figure 4. Masses indicate that tetramers and tetrameric oligomers of wild-type p53 bind and loop DNA. STEM mass thickness distinguishes two types of p53 assemblies: tandem tetramers aligned along the DNA and tetramers, in stacks, aligned perpendicular to the DNA. Tandem arrangement of tetramers reflects our use of multiple human genomic p53 recognition elements. Stacked tetramers arise from quaternary interactions among tetramers.

The histogram, which extends to 750 kDa, shows peaks at 1–4× the lowest mass. Additional masses beyond 750 kDa are not shown. In the inset at the right, the mean mass of each peak plotted versus oligomer number gives a straight line whose slope, 43 ± 3 kDa, is the monomer unit mass. Since mass peaks are integer multiples of four monomer unit masses, the mass data indicate that the tetramer found in solution also binds DNA as tetramers and multiples of tetramers.

In STEM images of tandem oligomeric masses, substructure that can be related to tetramer structures is visible. The appearance of most single tetramers observed at 13RE sites corresponded with the tetramer images shown in Figures 3A and 4A. Mass thickness in 40 out of 63 tandem oligomers observed, including the 8mer and 12mer and possibly the 16mer in Figure 4A, can be understood as mass contours of individual tetramers with some overlaps between adjacent tetramers due to close-spaced binding sites.

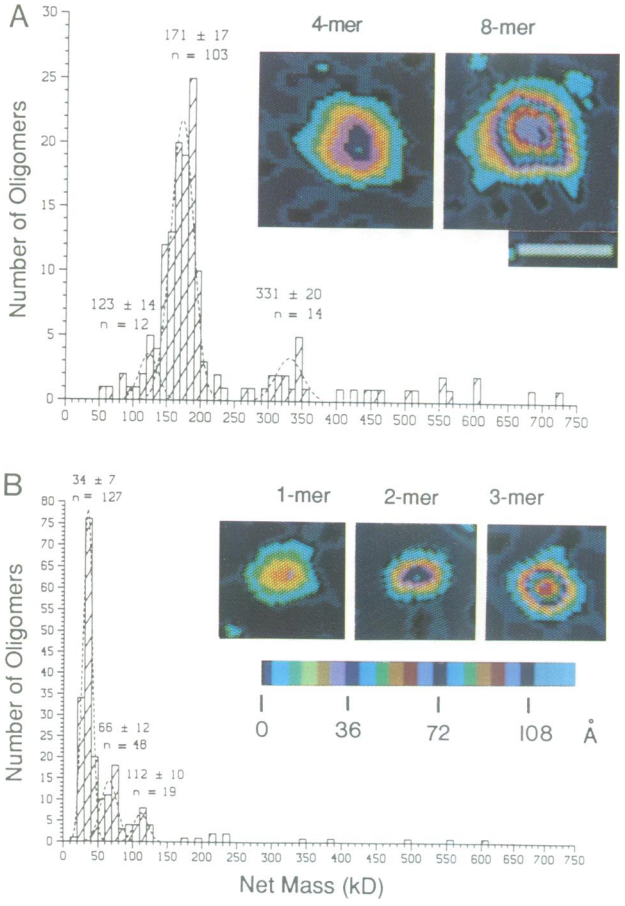

Fig. 3. Identification of oligomeric states of (**A**) p53 and (**B**) p53(1–320) in the absence of DNA by STEM mass measurements. Means ± SD are given for Gaussian distributions fitted to the main peaks in (A) and (B). Note that in (B) the *y*-axis has been compressed. Typical oligomeric structures in insets are shown as color representations of the scattered electron counts for each 10 $Å^2$ element. For each 5 count increase above the carbon film count, equal to 500 D/1.00 nm^2, the micrographs change color (Mastrangelo *et al.*, 1989). Since the partial specific volume for compact protein (0.75 cm^3/g) equals 800 D/nm^3 each color change is equivalent to (500/800) nm or 6 Å of compact protein. As shown in the color bar in (B), each color cycle between purple bands represents compact protein increments of 36 Å. Above 108 Å, gray replaces colors. In the second color cycle, red replaces pink to denote higher masses. Mass contours in a majority of p53 and p53(1–320) oligomers are consistent with those shown. Bar represents 10 nm.

Oligomerization by tetramer stacking observed in the absence of DNA also occurred at 13RE binding sites. Examples of stacked assemblies on DNA are shown in Figure 4B. The tandem 8+8mer of Figure 4A is reproduced here on the left at the scale of Figure 4B for comparison. Four tetramers lie side-by-side as two octamers along the DNA. In the 8mer stacked on 8mer in the center, two tandem tetramers each associate with a superposed tetramer. The 8mer stacked on 8mer reaches twice the mass thickness and contacts half the DNA length of the tandem 8+8mer. On the right, additional layers of tetramer stacking are evident in the 40mer intersite link structure whose mass thickness reaches the maximum coded (gray) level. Similarly stacked tetramers may account for the high-mass structures at many other loop junctures, including links between separated 20 bp p53CON sites (Figure 2D).

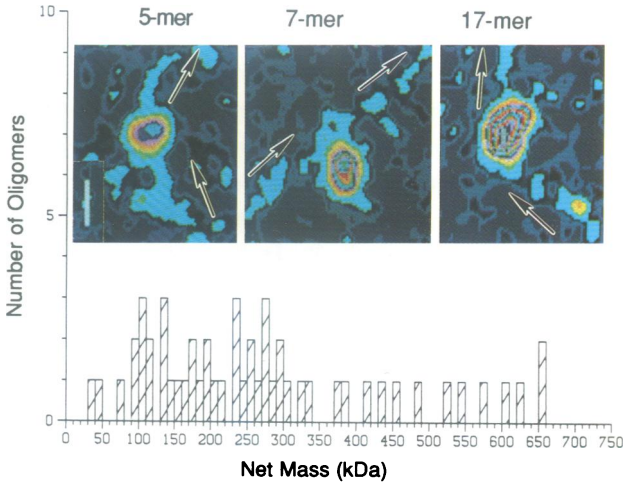

Fig. 5. STEM mass measurements identify p53(1–320) random oligomers as DNA binding forms. Histogram shows masses of both linked and unlinked complexes on *Hha*I–p13RE$^{PROX/DIST}$ fragments, minus the mass of DNA length contacted. Arrows indicate the DNA and, in some cases, a probable path through the complex. Fewer p53(1–320) than wild-type complexes were observed, presumably due to a reduced binding efficiency, and these low numbers were not sufficient for statistical analysis. Masses measured for the three oligomers shown in the inset are expressed as multimers of a 34 kDa monomer (Figure 3B) with an error estimated at <10%.

Stacked oligomers of p53(1–320) assemble at 13RE sites

The mass histogram for p53(1–320) complexed with 13RE sites shows a continuum of masses from monomer through 20mer (Figure 5) and beyond (data not shown). At the low end, only trimer masses form a minor group. The absence of favored oligomers suggests that p53(1–320) monomers or random combinations of monomers, dimers, and trimers combine with 13RE DNA. The mass of p53(1–320) multimers, such as the 5mer, 7mer and 17mer shown in insets in Figure 5, generally extends longitudinally along the DNA. Yet, even in the case of smaller oligomers such as the 7mer, mass thickness is characteristically greater than mass thickness observed for wild-type p53 oligomers of comparable mass. In the 17mer, mass thickness approaches the maximum (gray) level. These oligomers appear to assemble, in part, by stacking of multiple monomer masses similar to the p53(1–320) trimers observed in the absence of DNA (Figure 3B). p53(1–320) binding to consensus sequences may promote multiple stacking by monomer subunits. Intrasite and intersite loops might then form as a consequence of the additional DNA binding domains available.

Proximal and distal 13RE sites synergistically enhance transcription

To test whether long-range 13RE link structures affect p53-induced transcription *in vivo*, we compared chloramphenicol acetyltransferase (CAT) expression by promoters with 13REs located both proximal and distal to the *CAT* gene or at either site (Figure 6).

We cotransfected reporter plasmids with plasmids that expressed wild-type p53 or p53(1–320) under control of a cytomegalovirus (CMV) promoter. No CAT activity was detected in the presence of the control plasmid, pCMH6K, which did not express either protein (bars 1 and 2).

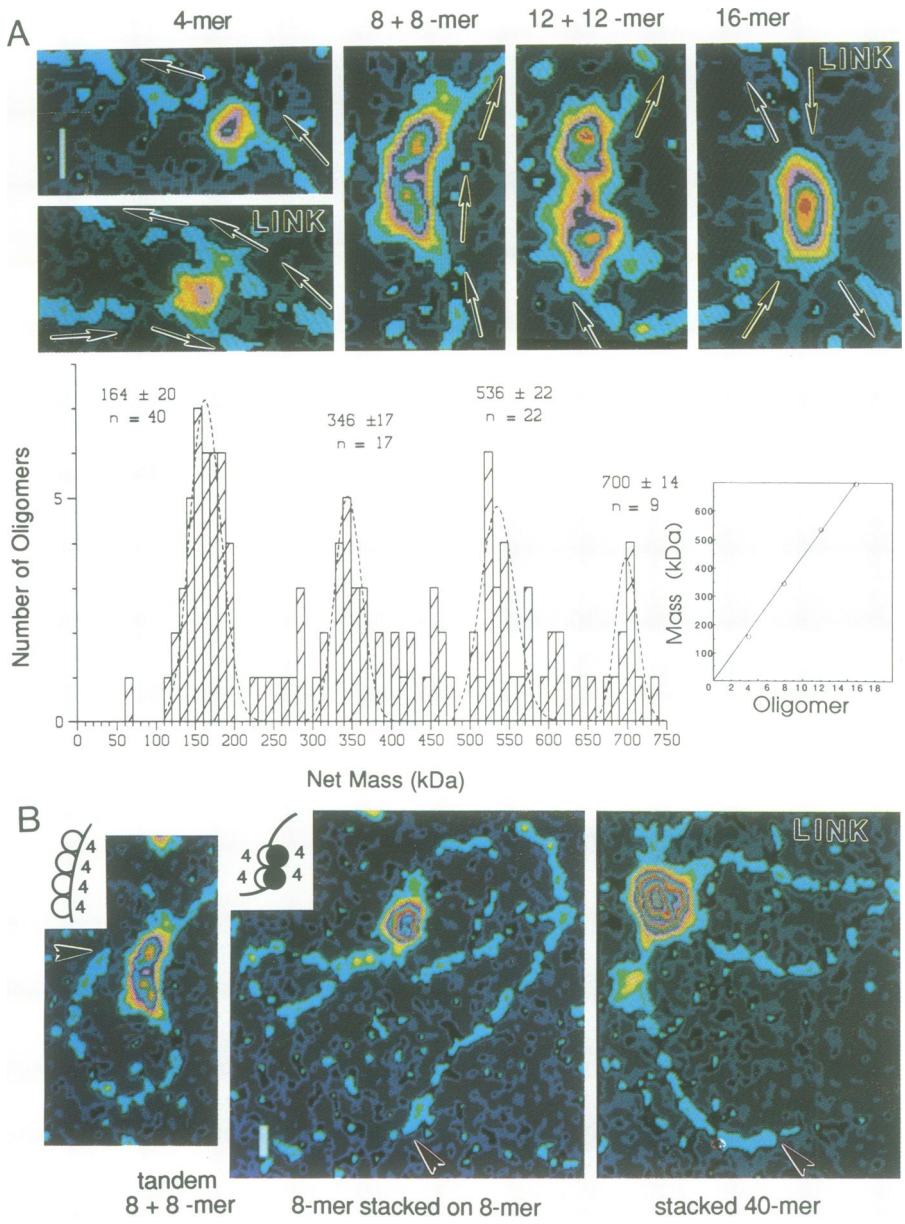

Fig. 4. STEM mass measurements identify tetrameric oligomers of wild-type p53 as DNA binding forms. The histogram shows masses of both linked and unlinked complexes on *Hha*I−p13RE$^{PROX/DIST}$ fragments minus the mass of DNA length contacted. Arrows show the DNA as it approaches complexes and, in some cases, a probable path through the complex. (**A**) Means of Gaussians fitted to mass peaks are plotted versus oligomer number in the inset at the right. The slope of the least squares fit line is 43 ± 3 kDa. Tandem tetramer structures, including two DNA loops labeled 'link', are displayed above the 4, 8, 12 and 16mer peaks and are discussed in the text. The bar represents 10 nm. (**B**) p53 tetramers form stacked structures at 13RE sites. In the left and center panels, the molecular mass of the tandem 8 + 8mer and the stacked 8mer on 8mer each measured 700 kDa. In insets, diagrams depict how four component tetramers in the tandem and in the stacked complexes might be arranged. In the right panel, a stacked 40mer forms an intersite loop. Arrowheads mark proximal ends of DNA fragments. The bar represents 10 nm.

Representative wild-type p53 and p53(1–320) expression levels for these experiments are shown in the inset in Figure 6. When p53 was expressed in the presence of TATA, but in the absence of 13RE sequences, CAT activity remained at background levels, ~570 c.p.m. (bars 3 and 4). p53 increased CAT activity 6-fold above background in the presence of a distal 13RE and 135-fold in the presence of a proximal 13RE (bars 5 and 6). p53(1–320) stimulated CAT activity 30-fold in the presence of a proximal 13RE and activity remained at background levels in the presence of the distal 13RE (bars 9 and 8). The lower transactivation capacity of p53(1–320) overall probably reflects a lower specific binding affinity apparent in the EM study. With both proximal and distal 13REs present, transcription was enhanced distinctly beyond the sum of individual transactivations (bars 7 and 10). The enhancement can be evaluated on comparing activation by distal elements in the absence and presence of proximal elements. Distal activation by wild-type protein is 25-fold higher in the presence of proximal sites than in their absence.

Although Kern *et al.* (1992) have shown that increasing the number of RGC sites increases the level of transactivation by p53, transcriptional enhancement by separated binding sites has not been demonstrated previously. It is formally possible that distal p53 potentiates proximal

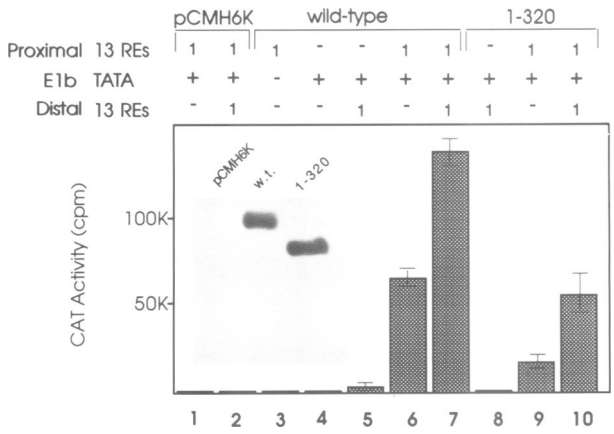

Fig. 6. p53 and p53(1–320) activate *CAT* gene expression synergistically when both proximal and distal 13RE binding sites are present. H358 cells, lacking endogenous p53, were transfected with *CAT* gene reporter plasmids that contained the E1b TATA and 13RE sequences either adjacent to TATA, or 1700 bp downstream from TATA, or at both sites (Figure 1A). The bars show levels of CAT activity induced by p53s expressed from co-transfected plasmids. In the inset, expression of p53 and p53(1–320) protein in H358 cells is shown. Proteins were concentrated by metal-affinity precipitation, analyzed by polyacrylamide gel electrophoresis and immunoblotting, and visualized by chemiluminescence.

activation rather than the reverse. The experimental observation of DNA looping suggests the simpler model—that the presence of proximal p53 potentiates distal p53 by retaining it at the local promoter. We conclude that formation of p53 and p53(1–320) link structures between proximal and distal response elements provides a physical basis for the synergistic stimulation of transcription.

One p53 tetramer combines with one consensus sequence site

The 20 bp palindromic consensus sequence for p53 DNA recognition consists of two repeated half sites, and each half site has two imperfect, inverted pentamer repeats. The consensus sequence, therefore, has either a bipartite or a quadripartite character. The binding unit responsible for recognition at the consensus sequence has not been established. Recent reports have implicated either the dimer (Hupp *et al.*, 1992; Tarunina and Jenkins, 1993) or the tetramer (Halazonetis *et al.*, 1993; Cho *et al.*, 1994; Hainaut *et al.*, 1994) as the p53 binding unit. STEM structures of known molecular masses arrayed at tandem binding sites provided a quantitative assay to assess the relationship between p53 quaternary structure and DNA target size. The relationship between mass bound in complexes and DNA length contacted by them reveals the protein:DNA-length stoichiometry.

To minimize ambiguities, we measured structures with mass thickness corresponding to the tetramer or tandem tetramers bound to relatively straight DNA (Figure 7). Stacked complexes were not included. Taking the DNA as a straight line through complexes in STEM micrographs, total lengths of *Hha*I DNA measured within 2% of the 2519 bp DNA sequence length. The greater accuracy of STEM compared to conventional EM length measurements of DNA has been noted previously (Hough *et al.*, 1982). In Figure 7, we plotted measured masses in monomer units versus bp of DNA covered. A regression line was

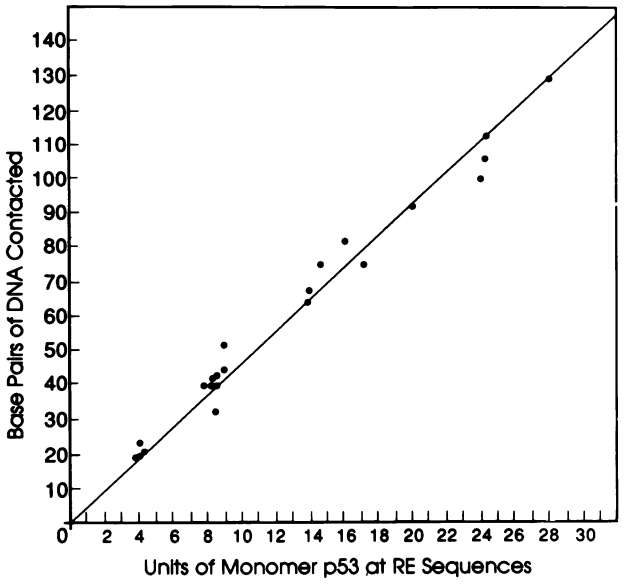

Fig. 7. One p53 tetramer contacts one consensus binding site. DNA lengths contacted by oligomeric masses were measured on complexes lying on relatively straight DNA. The unit for the abscissa is 43 kDa, the monomer mass derived from the mass ladder in Figure 4. The slope of the least squares fit line is 18.5 ± 1 bp per four monomer units and is in good agreement with the contact lengths measured for individual tetrameric structures.

fitted to the data by least squares. The slope of the line, 18.5±1 bp per four monomers, indicates that one tetramer interacts with one consensus sequence.

Discussion

We find that p53 can assemble oligomers by two distinct interactions. We and others have shown that the C-terminus has a strong autonomous tetramerization domain (Pavletich *et al.*, 1993; Clore *et al.*, 1994; Wang *et al.*, 1994). Our present results indicate that p53 has a non-tetrameric oligomerization domain(s) within amino acids 1–320. Together these domains account for the assembly of wild-type p53 tetramers from monomers, and the association of multiple tetramers by additional protein−protein interactions which we call stacking. Our studies implicate both oligomerization domains in transactivation.

Clues to mechanisms by which activator proteins function to regulate transcripton from basal promoters are steadily emerging. A general hypothesis proposes that synergy of gene activation is accomplished by combinations of activators or by multiple copies of a particular activator but rarely by a single activator molecule (Ondek *et al.*, 1988; Ptashne and Gann, 1990; Hori and Carey, 1994). Our present studies identify three potential mechanisms for presenting multiple copies of p53 for interaction with basal transcription complexes at the TATA sites in promoters. First, p53 tetramers are optimal consensus sequence binding forms. Each subunit of a p53 tetramer would contribute a strong N-terminal, acidic activation domain to the transcription complex. Second, p53 tetramers stack on tetramers at p53 binding sites. Our data are consistent with the idea that DNA binding actually promotes stacking of p53; larger p53 oligomers are found on DNA than are found free of DNA in our electron

micrographs. Alternatively, multiples of tetramers may be a preferred DNA binding form. Finally, p53 tetramers at distal binding sites can be translocated to proximal sites by protein−protein interactions among stacked tetramers. Stable protein−protein mediated DNA loops provide a general mechanism by which distant DNA sites modulate gene expression by bringing additional regulatory proteins to the vicinity of the TATA initiation complex (Bellomy and Record, 1990).

Tetramerization: p53 tetramers at consensus sites and separated response elements

Because specific binding by p53(1–320) to DNA is less efficient than that of wild-type p53, a major function of tetramerization may be to optimize affinity for the consensus sequence. Abundant single tetramers observed at DNA consensus sites and the stoichiometry of one tetramer to one consensus sequence indicate that a single tetramer is sufficient for stable binding at a consensus site.

Since we do not know the precise path of DNA in p53 complexes, the one tetramer:one consensus sequence stoichiometry can be interpreted in two ways. Four monomers of the tetramer bind the four quarter sites of the consensus sequence, a natural hypothesis (Funk *et al.*, 1992; Vogelstein and Kinzler, 1992). A model based on the co-crystal structure of the core DNA binding domain with several pentamer sequences proposes this geometry (Cho *et al.*, 1994). Alternatively, two monomers of the tetramer might interact with the two half sites of the consensus sequence leaving two monomers free to interact with a second consensus binding site. We have observed one example in its simplest form of a tetramer able to bind and link two separated DNA consensus sequences. The link tetramer in Figure 4A forms an intrasite loop and binds consensus sites apparently along opposite sides of the tetramer. In the link tetramer, contact with the separated consensus site can be via specific DNA binding domains in a free dimer half (Bargonetti *et al.*, 1993; Pavletich *et al.*, 1993; Wang *et al.*, 1993) or via non-specific DNA binding domains in the tetramer (Wang *et al.*, 1993). Supporting the idea that dimer halves might be functional subunits, artificial dimers of p53 have been found to activate transcription in a sequence-specific manner and to suppress growth of transformed cells (Pietenpol *et al.*, 1994). Future X-ray crystallographic studies of tetramer−DNA complexes will delineate the geometry of protein subunits at the consensus sequence.

Non-tetrameric oligomerization: stacking and DNA looping

In p53 tetramer stacks, one tetramer binds to a consensus sequence, tethering multiple activation and DNA binding domains of component tetramers to a single consensus site. Stacking between wild-type p53 tetramers appears qualitatively similar to stacking between monomers of p53(1–320), which lacks the C-terminal tetramerization domain. Further, stacked complexes of wild-type and tetramerization-deficient p53s both link well-separated proximal and distal promoter sites as distinct loop structures that are associated with enhanced transcription. These results and additional studies (Wang *et al.*, 1994) demonstrate the existence of a second, non-tetrameric oligomerization function residing in amino acids 1–320.

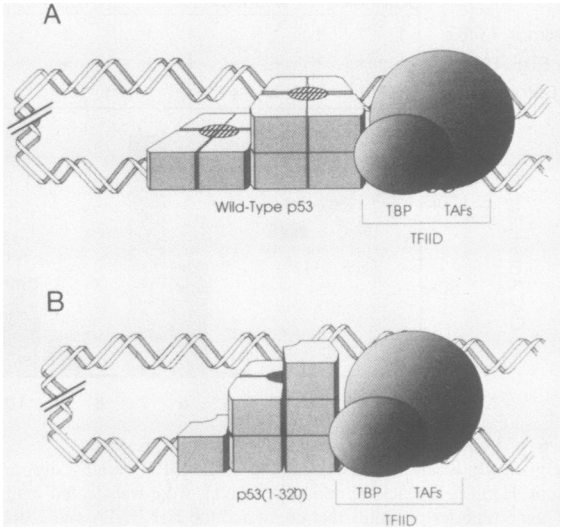

Fig. 8. Models represent the relationship of (**A**) wild-type p53 and (**B**) p53(1–320) oligomerization to looping and to transactivation. Tandem proteins (aligned along DNA) and stacked proteins (arranged perpendicular to DNA) are depicted in loop structures. In (A), C-terminal tetramerization domains appear as striped segments. Models include TBP and the TFIID accessory factors (TAFs). Details are found in the Discussion.

In the case of wild-type p53 tetramers, the tetramerization domain (Clore *et al.*, 1994) and side-to-side contacts between monomer subunits (Cho *et al.*, 1994) would stabilize tetrameric structure. By analogy with protein crystal structures (Almassy *et al.*, 1986; Johnson and Barford, 1990), additional top-to-bottom subunit contacts would keep two or more p53 tetramers stacked in register as multiples of tetramers. Interestingly, a segment of p53 consisting of amino acids 280–390 assembles tetramers but not larger oligomeric structures (Wang *et al.*, 1993). This observation suggests that the C-terminal tetramerization domain lacks significant top-to-bottom contacts. The (1–320) segment of p53, therefore, may provide top-to-bottom contacts in stacked wild-type molecules.

Although oligomers of p53(1–320) are relatively infrequent in the absence of DNA, STEM demonstrated assembly of large oligomeric structures extending along DNA in 13RE sites as highly stacked masses. Contact with the consensus site DNA may induce protein−protein interactions by aligning monomers of p53(1–320) in an arrangement similar to that normally present in tetramers, or by inducing conformational changes in bound subunits (Halazonetis and Kandil, 1993; Halazonetis *et al.*, 1993; Hainaut *et al.*, 1994), or by other mechanisms. These side-to-side interactions on DNA may enhance top-to-bottom interactions intrinsic to p53(1–320).

Model relating p53 oligomerization interactions with transactivation

p53 has been shown to bind via its activation domain directly to the TATA box binding polypeptide (TBP) of the basal transcription factor TFIID and to stabilize the TBP−TATA complex (Seto *et al.*, 1992; Chen *et al.*, 1993; Liu *et al.*, 1993; Martin *et al.*, 1993; Ragimov *et al.*, 1993; Truant *et al.*, 1993). A weak interaction with TFIIB has also been detected (Liu *et al.*, 1993). p53 tetramers

bound to proximal sites adjacent to the TATA sequences would be sufficient to accomplish transactivation functions at a basal level. Stacking associations among tetramers would increase the number of p53 activation domains at promoters. Furthermore, stacked wild-type p53 tetramers bound to proximal response elements would also provide additional opportunities for interactions with p53 bound to distal response elements and for translocation of that p53 to the TATA region by formation of DNA loops (Figure 8A). Together, these interactions might enhance basal transcripition in different ways. DNA loop structures may stabilize the binding of tetramers to recognition elements. Alternatively, multiple tetramers stacked at a proximal response element or in loop structures would maximally concentrate p53 and perhaps other transcriptional activators at the promoter. Both changes would increase the probability for interaction with TBP and TBP-associated factors (TAFs) and other basal transcription factors such as TFIIB. Because the basal transcription machinery appears capable of interacting with multiple activators (Hori and Carey, 1994), additional p53 molecules may yield additional active transcription complexes. Studies of Sp1 provide a precedent for the role of tetramer stacking and DNA looping in the synergistic activation of transcription (Mastrangelo *et al.*, 1991; Pascal and Tjian, 1991; Su *et al.*, 1991). The non-tetrameric oligomerization of p53(1–320) subunits would provide less efficient but analogous functions. Figure 8B shows how multiple p53(1–320) subunits might oligomerize and join separated DNA sites at the proximal promoter region.

Our studies of the role of p53 oligomerization in transactivation using model promoters provide a logical basis for exploring the interactions of p53 with natural but more complex promoters in cells.

Materials and methods

Protein expression and purification

Wild-type murine p53 was overexpressed in Sf9 insect cells using a baculovirus expression vector, then immunoaffinity purified and eluted with a decapeptide containing the pAb421 antibody epitope (Stenger *et al.*, 1992). Truncation mutant p53(1–320) was expressed in Sf9 cells using a similar baculovirus expression vector which adds six histidines to the N-terminus for purification by metal-affinity chromatography (Wang *et al.*, 1993). Construction of expressor plasmids pCMH6K, pCMH6Kp53 (wild-type), and pCMH6Kp53(1–320) used in animal cell transfection experiments has been described (Wang *et al.*, 1993). The CMV immediate-early promoter regulates transcription of the p53 and p53(1–320) proteins containing a 26 amino acid, N-terminal tag encoding six histidines, the hemagglutinin epitope and a recognition site for heart creatine kinase.

Plasmids

Reporter plasmids p13RE$^{PROX/DIST}$, p13RE^{PROX}, p13RE^{DIST} and control plasmids were derived from the pChlorAce-Basic(B) CAT vector (United States Biochemical) by adding the adenovirus 2 E1b TATA sequence and one or two copies of 13RE sequences. A synthetic E1b TATA sequence was inserted between the *Sal*I and *Xba*I sites upstream of the *CAT* gene. The 13RE sequence, from pPG$_{13}$-CAT (Kern *et al.*, 1992), was inserted between *Hin*dIII and *Pst*I sites, 25 bp upstream of the TATA sequence. The distal 13RE sequence was inserted into the *Bam*HI site using *Hin*dIII–*Bam*HI and *Bam*HI–*Pst*I linkers.

pJSJS was constructed from pBluescript KS (Stratagene) by inserting one copy of the p53 consensus sequence, p53CON, identified by Funk and colleagues (Funk *et al.*, 1992), between the *Bam*HI and *Pst*I sites and a second copy at the *Ssp*I site using blunt end ligation. All plasmids were sequenced to verify insertions and were purified using cesium chloride centrifugation.

Binding reactions, conventional EM and STEM

Plasmid DNAs were purified by cesium chloride centrifugation and, following restriction digestion, were phenol extracted and ethanol precipitated. The *Hha*I–pRE13$^{PROX/DIST}$ fragment was separated on a 5% polyacrylamide gel, visualized by long wavelength UV shadowing, eluted and cleared of acrylamide as described previously (Mastrangelo *et al.*, 1993). pJSJS was nicked by heating in 10 mM Tris–HCl, pH 8.0, 1 mM EDTA, and 200 mM NaCl at 75°C for 16 h. Binding buffer consisted of 20 mM Tris–HCl, pH 7.3, 100 mM NaCl, 5 mM DTT, and 10% glycerol. For wild-type p53, concentrations of different DNAs in reactions were varied, keeping a stoichiometry of 25 p53 monomers to one DNA template. In p53(1–320) reactions, the stoichiometry was 50 monomers to one DNA. 100 ng of wild-type p53 was added to 300 ng of *Aff*III–p13RE$^{PROX/DIST}$, 150 ng of *Hha*I–p13RE$^{PROX/DIST}$, or 180 ng of pJSJS. 160 ng of p53(1–320) was added to DNAs at the same concentrations. At higher protein concentrations, excess protein found on the thin carbon substrate seriously interfered with DNA visibility. Reactions were incubated for 30 min on ice. Glutaraldehyde was added to a concentration of 0.5% for 2 min. The reaction was immediately brought to 10 mM $MgCl_2$, and a 5 μl aliquot removed. We found comparable DNA binding, looping frequencies and measured masses using no glutaraldehyde, 0.5% glutaraldehyde crosslinking for 2 min, or 0.1% glutaraldehyde treatment for 15 min at room temperature. In conventional EM and STEM, protein structure was better preserved following the shorter glutaraldehyde treatment. We used the same conditions for mass measurements in the presence and absence of DNA.

As previously described, aliquots from reactions were adsorbed onto titanium grids that had been discharged in air and coated with poly-L-lysine. After washing with 20 mM ammonium acetate, EM grids were stained with uranyl acetate and shadowed with tungsten, while STEM grids were plunged into liquid N_2, followed by overnight sublimation (Mastrangelo *et al.*, 1993). EM and STEM grids were made, in parallel, from the same reactions. Experiments were repeated twice with similar results.

Principles of STEM mass measurement and data analysis have been described (Hough *et al.*, 1984; Mastrangelo *et al.*, 1989). Briefly, in high resolution STEM, a 3 Å diameter electron beam scans protein and DNA on a thin carbon substrate in a 10 Å^2 raster pattern. The number of electrons scattered by a molecule is proportional to the mass of constituent elements. During scanning, even at our relatively low doses, the electron beam will break covalent bonds and cause some mass rearrangements. Mass measurements remain sound since internal calibration procedures compensate for any mass loss.

CAT assays and immunoblotting

NCI-H358 human lung carcinoma cells that express no endogenous p53 (Funk *et al.*, 1992) were transiently transfected using DOTAP (Boehringer Mannheim) to deliver 5 μg each of the reporter and p53 expression plasmids, as has been described (Reed *et al.*, 1993). After 48 h, cells were washed twice with PBS, scraped, pelleted for 10 min at 4°C, and resuspended in 150 μl of 0.25 M Tris–HCl, pH 8.0. In reactions containing 50 μg of lysate protein, CAT activities were measured by phase extraction following procedures in the US Biochemical kit. Each assay was repeated four times.

We followed previously described procedures for concentrating and immunoblotting p53 proteins (Wang *et al.*, 1993). H358 cells in two 10 cm plates were transfected with 7.5 μg of pCMH6K plasmid DNAs expressing wild-type p53 or p53(1–320) using DOTAP. Tagged proteins in 0.5 ml lysis buffer were bound to 100 μl of Ni-NTA–agarose (Qiagen, Inc.) overnight at 4°C. Following washing with lysis buffer, the tagged p53s were released with 100 μl of SDS loading buffer for gel electrophoresis. The SDS–polyacrylamide gel was immunoblotted using a kit for enhanced chemiluminescence (Amersham) and a monoclonal antibody, 12CA5 (BABCO) in ascites fluid, which recognizes the hemagglutinin epitope carried on the N-terminal tag.

Acknowledgements

We thank Stan Fields, Patrick Hearing and Carl Anderson for helpful comments on the manuscript. This investigation was supported by Public Health Service grants NIH CA-28148 and NIH CA-18808, awarded by the National Cancer Institute (PT) and by the Department of Energy, Office of Health and Environmental Research (IAM, PVCH). We thank Joe Wall, director of the Brookhaven STEM, for his unfailing support. The STEM is an NIH Biotechnology Resource, RR0177.

References

Almassy,R.J., Janson,C.A., Hamlin,R., Xuong,N.H. and Eisenberg,D. (1986) *Nature*, **323**, 304–309.

Bargonetti,J., Friedman,P.N., Kern,S.E., Vogelstein,B. and Prives,C. (1991) *Cell*, **65**, 1083–1091.

Bargonetti,J., Manfredi,J.J., Chen,X., Marshak,D.R. and Prives,C. (1993) *Genes Dev.*, **7**, 2565–2574.

Beachy,P.A., Varkey,J., Young,K.E., VonKessler,D.P., Sun,B.I. and Ekker,S.C. (1993) *Mol. Cell. Biol.*, **13**, 6941–6956.

Bellomy,G.R. and Record,M.,Jr. (1990) *Prog. Nucleic Acid Res. Mol. Biol.*, **39**, 81–128.

Chen,X., Farmer,G., Zhu,H., Prywes,R. and Prives,C. (1993) *Genes Dev.*, **7**, 1837–1849.

Cho,Y., Gorina,S., Jeffrey,P.D. and Pavletich,N.P. (1994) *Science*, **265**, 346–355.

Clore,G.M., Omichinski,J.G., Sakaguchi,K., Zambrano,N., Sakamoto,H., Appella,E. and Gronenborn,A.M. (1994) *Science*, **265**, 386–391.

El-Deiry,W.S., Kern,S.E., Pietenpol,J.A., Kinzler,K.W. and Vogelstein,B. (1992) *Nature Genet.*, **1**, 45–49.

El-Deiry,W.S. *et al.* (1993) *Cell*, **75**, 817–825.

Farmer,G., Bargonetti,J., Zhu,H., Friedman,P., Prywes,R. and Prives,C. (1992) *Nature*, **358**, 83–86.

Fields,S. and Jang,S.K. (1990) *Science*, **249**, 1046–1049.

Foord,O., Bhattacharya,P., Reich,Z. and Rotter,V. (1991) *Nucleic Acids Res.*, **19**, 5191–5198.

Friedman,P.N., Chen,X., Bargonetti,J. and Prives,C. (1993) *Proc. Natl Acad. Sci. USA*, **90**, 3319–3323.

Funk,W.D., Pak,D.T., Karas,R.H., Wright,W.E. and Shay,J.W. (1992) *Mol. Cell. Biol.*, **12**, 2866–2871.

Ginsberg,D., Mechta,F., Yaniv,M. and Oren,M. (1991) *Proc. Natl Acad. Sci. USA*, **88**, 9979–9983.

Hainaut,P., Hall,A. and Milner,J. (1994) *Oncogene*, **9**, 299–303.

Halazonetis,T.D. and Kandil,A.N. (1993) *EMBO J.*, **12**, 5057–5064.

Halazonetis,T.D., Davis,L.J. and Kandil,A.N. (1993) *EMBO J*, **12**, 1021–1028.

Harper,J.W., Adami,G.R., Wei,N., Keyomarsi,K. and Elledge,S.J. (1993) *Cell*, **75**, 805–816.

Hollstein,M., Sidransky,D., Vogelstein,B. and Harris,C.C. (1991) *Science*, **253**, 49–53.

Hori,R. and Carey,M. (1994) *Curr. Opin. Genet. Dev.*, **4**, 236–244.

Hough,P.V.C., Mastrangelo,I.A., Wall,J.S., Hainfeld,J.F., Simon,M.N. and Manley,J.L. (1982) *J. Mol. Biol.*, **160**, 375–386.

Hough,P.V.C., Simon,M.N. and Mastrangelo,I.A. (1984) *Genet. Engng*, **6**, 279–307.

Hupp,T.R., Meek,D.W., Midgley,C.A. and Lane,D.P. (1992) *Cell*, **71**, 875–886.

Johnson,L.N. and Barford,D. (1990) *J. Biol. Chem.*, **265**, 2409–2412.

Kastan,M.B., Zhan,Q., El-Deiry,W.S., Carrier,F., Jacks,T., Walsh,W.V., Plunkett,B.S., Vogelstein,B. and Fornace,A.J.,Jr. (1992) *Cell*, **71**, 587–597.

Kern,S.E., Kinzler,K.W., Baker,S.J., Nigro,J.M., Rotter,V., Levine,A.J., Friedman,P., Prives,C. and Vogelstein,B. (1991a) *Oncogene*, **6**, 131–136.

Kern,S.E., Kinzler,K.W., Bruskin,A., Jarosz,D., Friedman,P., Prives,C. and Vogelstein,B. (1991b) *Science*, **252**, 1708–1711.

Kern,S.E., Pietenpol,J.A., Thiagalingam,S., Seymour,A., Kinzler,K.W. and Vogelstein,B. (1992) *Science*, **256**, 827–830.

Knight,J.D., Li,R. and Botchan,M. (1991) *Proc. Natl Acad. Sci. USA*, **88**, 3204–3208.

Li,R., Knight,J.D., Jackson,S.P., Tjian,R. and Botchan,M. (1991) *Cell*, **65**, 493–505.

Liu,X., Miller,C.W., Koeffler,P.H. and Berk,A.J. (1993) *Mol. Cell. Biol.*, **13**, 3291–3300.

Mack,D.H., Vartikar,J., Pipas,J.M. and Laimins,L.A. (1993) *Nature*, **363**, 281–283.

Martin,D.W., Munoz,R.M., Subler,M.A. and Deb,S. (1993) *J. Biol. Chem.*, **268**, 13062–13067.

Mastrangelo,I.A., Hough,P.V.C., Wall,J.S., Dodson,M., Dean,F.B. and Hurwitz,J. (1989) *Nature*, **338**, 658–662.

Mastrangelo,I.A., Courey,A.J., Wall,J.S., Jackson,S.P. and Hough,P.V.C. (1991) *Proc Natl Acad. Sci. USA*, **88**, 5670–5674.

Mastrangelo,I.A., Held,P.G., Dailey,L., Wall,J.S., Hough,P.V.C., Heintz,N. and Heintz,N.H. (1993) *J. Mol. Biol.*, **232**, 766–778.

Milner,J., Medcalf,E.A. and Cook,A.C. (1991) *Mol. Cell. Biol.*, **11**, 12–19.

Ondek,B., Gloss,L. and Herr,W. (1988) *Nature*, **333**, 40–45.

Pascal,E. and Tjian,R. (1991) *Genes Dev.*, **5**, 1646–1656.

Pavletich,N.P., Chambers,K.A. and Pabo,C.O. (1993) *Genes Dev.*, **7**, 2556–2564.

Pietenpol,J.A., Tokino,T., Thiagalingam,S., El-Deiry,W.E., Kinzler,K.W. and Vogelstein,B. (1994) *Proc. Natl Acad. Sci. USA*, **91**, 1998–2002.

Ptashne,M. (1986) *Nature*, **322**, 697–701.

Ptashne,M. and Gann,A.A.F. (1990) *Nature*, **346**, 329–331.

Ragimov,N., Krauskopf,A., Navot,N., Rotter,V., Oren,M. and Aloni,Y. (1993) *Oncogene*, **8**, 1183–1193.

Raycroft,L., Wu,H. and Lozano,G. (1990) *Science*, **249**, 1049–1051.

Reed,M., Wang,Y., Mayr,G., Anderson,M.E., Schwedes,J.F. and Tegtmeyer,P. (1993) *Gene Exp.*, **3**, 95–107.

Scharer,E. and Iggo,R. (1992) *Nucleic Acids Res.*, **20**, 1539–1545.

Seto,E., Usheva,A., Zambetti,G.P., Momand,J., Horikoshi,N., Weinmann,R., Levine,A.J. and Shenk,T. (1992) *Proc. Natl Acad. Sci. USA*, **89**, 12028–12032.

Shaulian,E., Zauberman,A., Milner,J., Davies,E.A. and Oren,M. (1993) *EMBO J.*, **12**, 2789–2797.

Shore,D., Langowski,J. and Baldwin,R.L. (1981) *Proc. Natl Acad. Sci. USA*, **78**, 4833–4837.

Stenger,J.E., Mayr,G.A., Mann,K. and Tegtmeyer,P. (1992) *Mol. Carcinog.*, **5**, 102–106.

Sturzbecher,H.-W., Brain,R., Addison,C., Rudge,K., Remm,M., Grimaldi,M., Keenan,E. and Jenkins,J.R. (1992) *Oncogene*, **7**, 1513–1523.

Su,W., Jackson,S., Tjian,R. and Echols,H. (1991) *Genes Dev.*, **5**, 820–826.

Tarunina,M. and Jenkins,J.R. (1993) *Oncogene*, **8**, 3165–3173.

Truant,R., Xiao,H., Ingles,C.J. and Greenblatt,J. (1993) *J. Biol. Chem.*, **268**, 2284–2287.

Unger,T., Nau,M.M., Segal,S. and Minna,J.D. (1992) *EMBO J.*, **11**, 1383–1390.

Vogelstein,B. and Kinzler,K.W. (1992) *Cell*, **70**, 523–526.

Wang,Y., Reed,M., Wang,P., Stenger,J.E., Mayr,G., Anderson,M.E., Schwedes,J.F. and Tegtmeyer,P. (1993) *Genes Dev.*, **7**, 2575–2586.

Wang,P., Reed,M., Wang,Y., Mayr,G., Stenger,J.E., Anderson,M.E., Schwedes,J.F. and Tegtmeyer,P. (1994) *Mol. Cell. Biol.*, **14**, 5182–5191.

Weintraub,H., Hauschka,S. and Tapscott,S.J. (1991) *Proc. Natl Acad. Sci. USA*, **88**, 4570–4571.

Wolffe,A.P. (1994) *Cell*, **77**, 13–16.

Wu,X., Bayle,J.H., Olson,D. and Levine,A.J. (1993) *Genes Dev.*, **7**, 1126–1132.

Zambetti,G.P., Bargonetti,J., Walker,K., Prives,C. and Levine,A.J. (1992) *Genes Dev.*, **6**, 1143–1152.

Received on August 4, 1994; revised on October 7, 1994